Electron and Mass Transport in Hybrid Redox Polyether Melts: Co and Fe Bipyridines with Attached Polyether Chains

Mary Elizabeth Williams, Hitoshi Masui, Jeffrey W. Long, Jitendra Malik, and Royce W. Murray*

Contribution from the Kenan Laboratories of Chemistry, University of North Carolina, Chapel Hill, North Carolina 27599-3290

Received July 23, 1996. Revised Manuscript Received October 7, 1996[⊗]

Abstract: The coupling of electron self exchange reactions with physical diffusion has been used to measure electron transfer rate constants in a series of undiluted metal complex molten salts $[M(bpy(CO_2MePEG)_2)_3](ClO_4)_2$ where M = Co(II/I) and Fe(III/II) and MePEG is an oligomeric polyether of MW 150, 350, and 550. Physical self-diffusion rates in the melts vary with attached polyether chain length by over 10^3-fold while the electron transfer rate constants show no strong systematic dependence. The electron transfer rates and activation parameters indicate that the metal complex cores move rapidly within their attached polyether "solvent" shells relative to the rates of electron transfers, which are near adiabatic with large activation barriers reflecting the apparent inability of the attached polyether chains to act as a freely mobile "solvent". Ionic conductivities of the melts were measured in order to inspect for ionic and electronic migration effects which are present to minor degrees. Diffusion and heterogeneous transfer rates are also reported for dilute solutions of the cobalt complexes in a polyether solvent.

Electron hopping in solid and semisolid materials is a fundamentally and technologically significant topic,[1] yet in comparison to the considerable literature on the molecular details of electron self exchange reactions in fluid solutions,[2] experimental evidence that delineates the molecular factors controlling solid state electron transfer dynamics is still quite limited. As part of our longstanding interest[3] in this subject, a structurally versatile class of highly viscous molecular melts has been synthesized based on attaching short polyether chains to normally crystalline redox moieties, and some electron transport results have been obtained.[3] Understanding of electron transfer in fluid solvents has classically been aided by observing the effects of structural variations. This report describes mass and electron transport measurements in *undiluted melts* of metal complex perchlorates in which the metals are Co and Fe and the ligand is bipyridine to which polyethers of different chain lengths (as designated in the structures) have been attached.

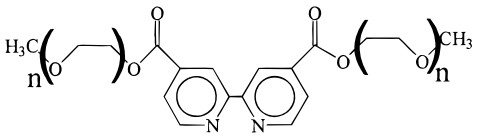

E3M : n = 3
MePEG-350: n = 7
MePEG-550: n = 11
MePEG-750: n = 15

When prepared in mixed valent form, as during voltammetry of the pure metal complex melts, the oxidized and reduced forms of the undiluted metal complexes are nominally in contact so that electron self exchanges may freely occur. The polyether chains are both part of the ligands of the metal complexes, and serve as a "solvent" shell whose properties may influence the dynamics of electron self exchanges between the oxidized and reduced complexes. The electron transfer centers are also, potentially, separated by their attached polyether chains. Even though temperatures above glassing and melting transitions are used, the melts are viscous semisolids so that physical diffusion of the metal complex centers is restrained. The parameters of this unique environment can be manipulated by varying the attached polyether chain length, providing a novel tool for investigation of the factors which control rates of electron transfer reactions. These complexes are also attractive in comparison to vinyl-substituted, electropolymerized metal bipyridine complexes,[4] where the environment of the redox centers is less readily controlled or manipulated. The results of this study indicate that the metal complexes move rapidly within their "solvent" shells relative to the frequency of electron

[⊗] Abstract published in *Advance ACS Abstracts,* February 1, 1997.

(1) For example: (a) Murray, R. W. *Molecular Design of Electrode Surfaces*; Murray, R. W., Ed.; John Wiley & Sons: New York, 1992. (b) Abruna, H. D. *Electroresponsive Molecular and Polymeric Systems*; Skotheim, T., Ed.; Marcel Dekker: New York, 1988. (c) Ratner, M. A.; Nitzan, A. *Faraday Discuss. Chem. Soc.* **1989**, *88*, 19. (d) Rosseinsky, D. R.; Monk, P. M. S. *J. Chem. Soc., Faraday Trans.* **1994**, *90*(8), 1127−31. (e) Facci, J. S.; Abkowitz, M.; Linburg, W.; Knier, F. *J. Phys. Chem* **1992**, *95*(120), 7908. (f) Mathias, M. F.; Haas, O. *J. Phys. Chem.* **1993**, *97*(36), 9217−25. (g) Bard, A. J. *Integrated Chemical Systems*, John Wiley and Sons: New York, 1994; pp 1−35. (h) Bottger, H.; Bryskin, V. V. *Hopping Conduction In Solids*; VCH Publishers: Deerfield Beach, FL, 19??; pp 218−236. (i) Ashwell G. J. *Molecular Electonics*; John Wiley and Sons: New York, 1992. (j) Hoffman, B. M.; Ratner, M. A. *Inorg. Chim. Acta* **1996,** *243,* 233.

(2) (a) Marcus, R. A. *Rev. Modern Phys*. **1993**, *65*, 599. (b) Marcus, R. A. *Angew. Chem*. **1993**, *32*, 1111. c) Marcus, R. A. *J. Phys. Chem*. **1995**, *99*, 5742. (d) Fawcett, W. R.; Opallo, M. *Angew. Chem*. **1994**, *33*, 2131. (e) Weaver, M. J. *Chem. Rev.* **1992**, *92*, 463. (f) Heitele, H. *Angew. Chem*. **1993**, *32*, 359. (g) Langen, R.; Chang, I. J.; Germanas, J. P.; Richards, J. H.; Winkler, J. R.; Gray, H. B. *Science* **1995**, *268*, 1733.

(3) (a) Long, J. W.; Velasquez, C. S.; Murray, R. W. *J. Phys. Chem.* **1995**, *100*, 5492. (b) Pyati, R.; Murray, R. W. *J. Am. Chem. Soc*. **1996**, *118*, 1743. (c) Velasquez, C. S.; Hutchinson, J. E.; Murray, R. W. *J. Am. Chem. Soc.* **1993**, *115*, 7896. (d) Hatazawa, T.; Terrill, R. H.; Murray, R. W. *Anal. Chem.* **1996**, *68*, 597. (e) Poupart, M. W.; Velasquez, C. S.; Hassett, K.; Porat, Z.; Haas, O.; Terrill, R. H.; Murray, R. W. *J. Am. Chem. Soc.* **1994**, *116*, 1165. (f) Terrill, R. H.; Hatazawa, T.; Murray, R. W. *J. Phys. Chem.* **1995**, *99*, 16676.

(4) (a) Sosnoff, C. S.; Sullivan, M. G.; Murray, R. W. *J. Phys. Chem.* **1994**, *98*, 13643. (b) Terrill, R. H.; Murray, R. W. In *Molecular Electronics*, Jortner, J.; Ratner, M. A., Eds.; Blackwell Science, IUPAC informal series Chemistry for the 21st Century Monographs, in press.

S0002-7863(96)02531-0 CCC: $14.00

transfers, and that the Co(II/I) and Fe(II/III) reactions are near adiabatic with large activation barriers, reflecting the apparent inability of the attached polyether chains to act (energetically) as a freely mobile "solvent".

The rate constants k_{EX} of homogeneous electron self exchange reactions in the metal complex melts can be assessed by voltammetry because electron transfers in the mixed valent layer around the microelectrode serve as a more efficient charge transport mechanism than physical diffusion of the metal complex sites themselves. The apparent diffusion coefficient, D_{APP}, for a voltammetric process that involves coupled electron hopping-physical diffusion is given by the Dahms−Ruff relation:[5]

$$D_{APP} = D_{PHYS} + \frac{k_{EX}\delta^2 C}{6} \quad (1)$$

where D_{PHYS} is the metal complex physical self-diffusion coefficient, and C and δ are the concentration and average center-to-center distances between the complexes in the melts which are evaluated from the melt densities. The right-hand term in eq 1 is termed the electron diffusion coefficient, D_E. Values of k_{EX}, as are their temperature dependencies, are evaluated with eq 1 from D_{APP} measurements for the Co(II/I) and Fe(III/II) couples in the melts. The D_{APP} of the relatively slowly electron exchanging Co(III/II) couple is used as a measure of D_{PHYS} of the M(II) state.[3a] Ionic conductivities of the melts are measured as supporting data and as a means of evaluating ionic and electronic migration effects, leading to a minor correction of electron diffusion coefficients and the rate constants calculated from them. These corrected values are labeled $D_{E,COR}$ and $k_{EX,COR}$, respectively.

Experimental Section

Reagents. 4-Picoline (Aldrich) was purified by distillation. The polyethylene oxide monomethyl ether samples with molecular weights M_N = 150, 350, 550, and 750 g/mol (E_3M, MePEG-350, MePEG-550, and MePEG-750, respectively, Aldrich) were dried under vacuum at elevated temperatures for at least 24 h before use. $Fe(ClO_4)_2 \cdot 6H_2O$ and $Co(ClO_4)_2 \cdot 6H_2O$ (Aldrich, used as received) were stored in a desiccator as was $LiClO_4$ (Aldrich) after recrystallization from methanol and drying under vacuum at 80 °C. Chromatography was performed using 60 Å pore 230−400 mesh silica gel (Baxter). Other reagents were used as received.

Preparation of Ligands. Using a catalytic amount of Pd on activated carbon, 4-picoline was coupled[6] to give 4,4′-dimethyl-2,2′-bipyridine, which was recrystallized from ethyl acetate, dried at 80 °C under vacuum for 12 h, and then oxidized with acidic $KMnO_4$ to 4,4′-dicarboxylic acid-2,2′-bipyridine.[7] The solid white acid was dried at 100 °C under vacuum for 24 h, and converted[8] to its acid chloride by refluxing in pure thionyl chloride for 48 h. Distilling excess thionyl chloride from the clear yellow solution, the product was recrystallized from heptane and dried in vacuo. The 4,4′-diacid chloride bpy was esterified with the desired polyethylene oxide methyl ether in benzene solution, using a mole ratio of less than 2:1 polyether to bpy, and the resulting di-tailed bpy ligand separated from incompletely reacted bipyridine by column chromatography on silica gel using acetone as eluent as described previously.[3a] Purity of the di-tailed bpy ligand was confirmed using ^{1}H NMR (Bruker AC-250 MHz NMR); the protons on the first ethylene oxide monomer unit (i.e., adjacent to the ester) are shifted slightly downfield, allowing their integration apart from the remainder of the polymer chain. The ratio of the area of these first four protons on the chain to that for the pyridine protons is 4:3 for pure, di-tailed ligand.

Preparation of Metal Complexes. An excess of di-tailed bpy ligand was reacted with $M(ClO_4)_2 \cdot 6H_2O$ (M = Fe or Co) in anhydrous methanol for at least 12 h. After removing the methanol (rotary evaporation), excess ligand was extracted from the highly viscous metal complex melt by repeated washing with carbon tetrachloride and ethyl ether, confirming purity of the product by ^{1}H NMR in its acetone solutions.[9]

The related complexes $[Co(bpy)_3](ClO_4)_2$ and [Co(2,2′-bipyridine-4,4′-ethyl ester)$_3$]$(ClO_4)_2$ were prepared by reacting 2,2′-bipyridine and 4,4′-ethyl ester-2,2′-bipyridine, respectively, with $Co(ClO_4)_2 \cdot 6H_2O$ in methanol, recrystallizing the product from methanol.

Electrochemical Measurements. Cyclic voltammetry and chronoamperometry of the undiluted metal complex melts were performed using a low-current potentiostat[10] capable of measuring currents in the tens of femtoampere range. Experiments were controlled using an IBM compatible computer equipped with a Keithley DAS-HRES 16-bit A/D board. The three-electrode assembly consisted, as previously noted,[11] of wire tips of a 25 μm diameter Pt working microelectrode, a 24 gauge wire Pt counter electrode, and a 0.5 mm wire Ag quasi-reference electrode exposed on a polished, insulating platform. The platform was polished with successively smaller grades (to 0.05 μm) of alumina and sonicated in ethanol prior to each use. Films of the metal complex melts (*ca*. 1 mm) were cast onto the platform in a sealed system and dried under vacuum at 75 °C for at least 12 h. Rigorous drying conditions are important since transport properties of the metal complex melts are sensitive to absorbed moisture. Films were equilibrated at each temperature (controlled using a Brookfield Model EX-100/ FTC-350A circulating bath and cooler) for at least 1 h prior to measurement, and all measurements are performed under active vacuum.

The ionic conductivities of the metal complex melts are small and necessitate slow potential scan rates in cyclic voltammetry to avoid distortions from uncompensated resistance. No $LiClO_4$ supporting electrolyte was added since added electrolytes strongly affect[3a] other properties of these melts (including D_{PHYS} and k_{EX}, as will be reported separately[12]) and may even depress (not increase) their ionic conductivities.[3a] D_{APP} values were measured by chronoamperometry (potential steps of 300−400 mV to the diffusion-limited region of the voltammetric wave) and current−time traces recorded for as long as 3000 s. The diffusion geometry is generally linear, but at longer times a mixed linear−radial diffusion geometry can potentially occur, so current−time curves were analyzed by iterative fitting to the Shoup−Szabo equation:[13a]

$$I = 4nFrD_{APP}C\left[0.7853 + \frac{0.8862}{t^{1/2}} + 0.2146\ \mathrm{EXP}\left(\frac{-0.7832}{t^{1/2}}\right)\right] \quad (2)$$

where I is current, F Faraday's constant, r the microelectrode radius, and t time.[13b]

Ionic conductivities of the melts were measured (Solartron Model SI 1260 Impedance Analyzer and 1267 Electrochemical Interface) as thoroughly dried (75 °C in vacuo for at least 12 h) films on an interdigitated array (IDA) electrode assembly consisting of 50 pairs of interdigitated Pt fingers, each 10 μm wide, 0.1 μm high, 2 mm long, and separated by 5-μm gaps. The IDA devices were generously donated by O. Niwa of Nippon Telephone and Telegraph. Impedance

(5) Majda, M. In *Molecular Design of Electrode Surfaces*; Murray, R. W., Ed.; John Wiley & Sons: New York, 1992; p 159.

(6) Sasse,W. H. F.; Whittle, C. P. *J. Am. Chem. Soc.* **1961**, *83*, 1347.

(7) Sprintschnik, G.; Sprintchnik, H. W.; Kirsch, P. P.; Whitten, D. G. *J. Am. Chem. Soc*. **1977,** *99*, 4947.

(8) Evers, R. C.; Moore, G. J. *J. Polym. Sci.* **1986**, *24*, 1863.

(9) Crooker, J. C., University of North Carolina at Chapel Hill, unpublished results, 1995.

(10) Woodward, S., University of North Carolina Department of Chemistry Electronics Consultant, design and construction.

(11) (a) Watanabe, M.; Wooster, T. T.; Murray, R. W. *J. Phys. Chem.* **1991**, *95***,** 45. (b) Wooster, T. T.; Longmire, M. L.; Watanabe, M.; Murray, R. W. *J. Phys. Chem.* **1991**, *95*, 5315.

(12) Williams, M. E., University of North Carolina at Chapel Hill, unpublished results, 1996.

(13) (a) Shoup, D.; Szabo, A. *J. Electroanal. Chem.* **1982**, *140***,** 237. (b) Under linear diffusion conditions (i.e., short time scales), the data are expected to follow the Cottrell equation, $i = nFAD^{1/2}C/\pi^{1/2}t^{1/2}$. The data were analyzed using both eq 2 and the Cottrell equation in order to consistently check for mixed diffusion geometries. The reported D is the average of these.

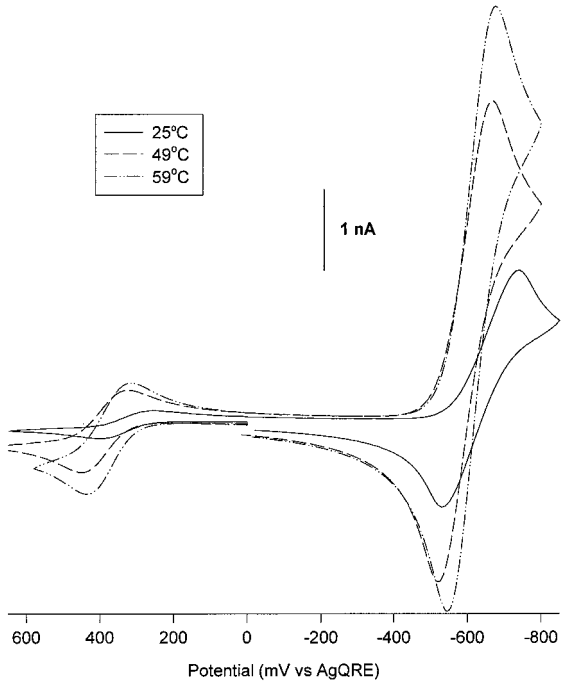

Figure 1. Cyclic voltammograms (5 mV/s) of undiluted [Co(bpy(CO_2-MePEG-350)$_2$)$_3$](ClO_4)$_2$ melt at a 12.5 μm radius Pt microdisk electrode at indicated temperatures.

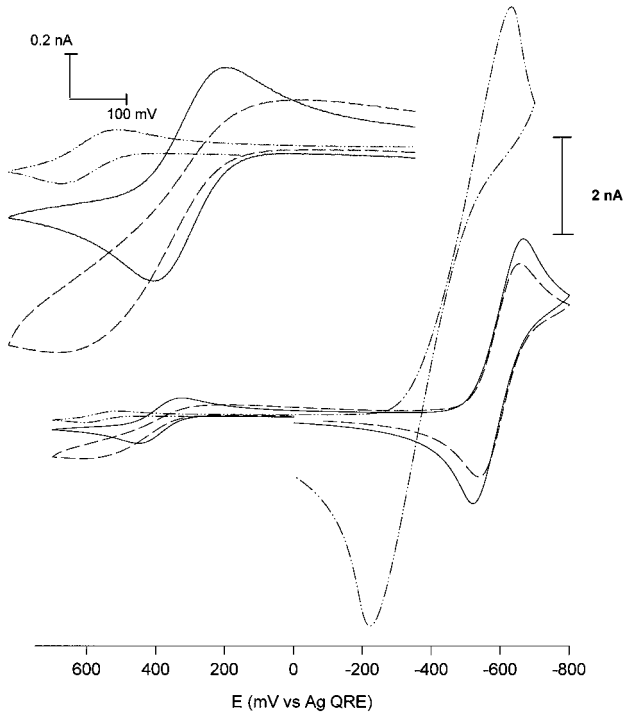

Figure 2. Cyclic voltammograms (5 mV/s) at 49 °C at a 12.5 mm radius Pt microdisk of the Co(III/II) oxidation and Co(II/I) reduction in undiluted [Co(bpy(CO_2E_3M)$_2$)$_3$](ClO_4)$_2$ (—••—), [Co(bpy(CO_2MePEG-350)$_2$)$_3$](ClO_4)$_2$ (—), and [Co(bpy(CO_2MePEG-550)$_2$)$_3$](ClO_4)$_2$ (— —) melts. The greater iR_{UNC} distortion in the Co(II/I) wave in the [Co(bpy(CO_2E_3M)$_2$)$_3$](ClO_4)$_2$ melt is due to the lower conductivity of that melt (Table 3). The inset is an expansion of the Co(III/II) waves.

measurements from 1 MHz to 1 Hz were performed at 0 V DC bias and 10−50 mV AC amplitude. The IDA cell constant was calibrated with a 1 M $LiClO_4$ solution of known conductivity in polyethylene glycol (M_N = 2000 g/mol). The IDA was mounted on a temperature-controlled stage[3f] (Lakeshore 330 Autotuning Temperature Controller) and maintained under vacuum.

Some voltammetric measurements were performed on dilute (5 mM) solutions of the Co complexes in the polymer electrolyte 1.5 M $LiClO_4$/MePEG-350 (16:1 ether oxygen−Li). These solutions were prepared using acetone as a casting solvent, which was removed by rotary evaporation followed by drying under vacuum for 24 h.

Error Analysis. The data have been analyzed for statistical validity using standard methods of error analysis.[14] For multiple measurements, the raw data reported as mean value (± standard error of mean) single measurements are reported as x (± uncertainty in x). All (subsequent) calculations include a propagation of errors from the raw values. Analyses of activation plots using either linear regression or nonlinear VTF fits (*vide infra*, Results and Discussion) include uncertainties in slopes and intercepts, taking into account errors in individual measurements, degrees of freedom, and the "goodness of fit" of the regression.

Other Measurements. Differential scanning calorimetric measurements were taken using a Seiko DSC 220-CU, at heating/cooling rates of 5 °C/min from −100 to 100 °C, under a stream of dry N_2. Samples were dried under vacuum at elevated temperatures in pre-weighed pans for 12 h prior to measurement. Viscosities of carefully dried 1-mL samples were obtained (under N_2) using a Brookfield Model DV-III programmable rheometer.

Results and Discussion

Voltammetry and Transport Measurements in Undiluted Metal Complex Melts. The undiluted metal complex melts are room temperature, intrinsically ionically conductive molten salts, and can be studied directly with microelectrode voltammetry. Unlike their dilute solutions in a polyether polymer electrolyte (*vide infra*, Table 5), the viscosity and transport properties of the undiluted metal complex melts are strongly dependent on the chain length of the polyether attached to the bpy ligand.

Figure 1 shows examples of cyclic voltammetry in the [Co(bpy(CO_2MePEG-350)$_2$)$_3$](ClO_4)$_2$ melt at various temperatures. The wave at positive potentials represents the Co(III/II) reaction and that at negative values the Co(II/I) reaction.[11] Even though the same complex—[Co(bpy(CO_2MePEG-350)$_2$)$_3$]$^{2+}$—physically diffuses to the electrode in both reactions, the reduction reaction yields much larger currents. Chronoamperometric measurements of reduction currents give a D_{APP} = 1.5 × 10^{-9} cm^2/s (25 °C) diffusion coefficient for Co(II/I) voltammetry in the [Co(bpy(CO_2MePEG-350)$_2$)$_3$](ClO_4)$_2$ melt. This D_{APP}, according to eq 1, is a composite of physical diffusivity (D_{PHYS}) and electron self exchange reactions (k_{EX}) in the Co(II/I) mixed-valent layer around the microelectrode.

The self exchange rate constant for Co(II/I) bipyridine in fluid solution is known to be large whereas that for the Co(II/III) reaction is very small.[15] Electron self exchange accordingly does not contribute to currents (Figure 1) for the oxidation of Co(II) in its melt, because the Co(III/II) electron transfer rate is insufficiently fast to do so. In dilute fluid solutions, the well-known Co(III/II) spin state transition supposedly slows its electron self exchange reactions,[15] and in dilute polyether solutions (*vide infra*, Table 5) they are even slower. (The difference between the Co(II/I) and Co(III/II) electron transfer rates for measuring k_{EX} was first exploited by Anson and Buttry, in a different context.[16]) Chronoamperometry of the Co(III/II) wave in Figure 1 gives a value of 1.3 × 10^{-11} cm^2/s (25 °C)

(14) Taylor, J. R. *An Introduction to Error Analysis, The Study of Uncertainties in Physical Measurements*, Oxford University Press: Oxford, UK, 1982.

(15) (a) Sutin, N.; Brunschwig, B. S.; Creutz, C.; Winkler, J. R. *Pure Appl. Chem.* **1988**, *60*, 1817. (b) k_{EX} = 1 × 10^9 and 18 M^{-1} s^{-1} for Co(II/I) and Co(III/II) of [Co(bpy)$_3$], respectively, in water. Co(III/II) k_{EX} is assumed to be 18 M^{-1} s^{-1}, then the largest D_E that can be calculated (using δ and C from Table 2), 3.8 × 10^{-14} cm^2 s^{-1}, is ∼10 times less than the smallest measured D_{PHYS}. Actually, based on heterogeneous rates (Table V), k_{EX} is orders of magnitude smaller in the metal complex melts than in aqueous solution.

(16) Buttry, D. A.; Anson, F. C. *J. Am. Chem. Soc.* **1983**, *105*, 685.

for $D_{APP} = D_{PHYS}$ of the $[Co(bpy(CO_2MePEG\text{-}350)_2)_3]^{2+}$ complex in its melt. This result applied to eq 1 with the Co(II/I) D_{APP} yields D_E, which after a small correction for an electronic migration effect (*vide infra*, Table 4) gives $D_{E,COR} = 1.2 \times 10^{-9}$ cm^2 s^{-1} and a Co(II/I) $k_{EX,COR} = 6.7 \times 10^5$ M^{-1} s^{-1} (25 °C).

Figure 2 shows voltammograms at 49 °C for the Co complexes as a function of their attached polyether chain lengths.[17] The currents for the Co(III/II) oxidations (and the associated D_{PHYS}) decrease with decreasing polyether chain length, and as in Figure 1, those for the Co(II/I) wave are much larger owing to contributions from electron self exchange reactions. D_{PHYS} (Co(III/II)) and D_{APP} (Co(II/I)) values measured at 25 °C with chronoamperometry are reported in Table 1 as are results[18] for D_E and $D_{E,COR}$. Table 2 gives 25 °C results for $k_{EX,COR}$ (which is $6D_{E,COR}/\delta^2C$) and Figure 3 (▲) shows activation plots of D_E ($=D_{APP} - D_{PHYS}$) from which the barrier energies $E_{A,ET}$ and intercepts $k_{EX}°$ in Table 2 for the Co(II/I) reaction were derived.

Voltammetry (not shown) of the Fe(III/II) wave in the Fe complex melts exhibits currents and corresponding D_{APP} values that are similar to those of Co(II/I) (see Table 1) and are likewise associated with electron self exchange. Since the Fe complexes are formally isostructural with the Co complexes, and δ values obtained from their melt densities are virtually identical, it seems reasonable to assume (as we have before[3a]) that D_{PHYS} values derived from the Co(II/III) voltammetry can be used to represent the D_{PHYS} of the Fe complex. This was done to produce the 25 °C D_E and $D_{E,COR}$ results in Table 1 and the $k_{EX,COR}$ data in Table 1 for the Fe(III/II) reaction. Table 1 also gives activation results for the Fe(III/II) reaction derived from the corresponding Arrhenius plots in Figure 3 (●).

The voltammetry of the MePEG-550 tailed Fe and Co complexes was not stable above *ca.* 35 and 50 °C, respectively, for unknown reasons, and given the small accessible temperature range, activation results for that Fe complex were judged not reliable. Likewise, for the MePEG-550 tailed Co complex, the difference between D_E and D_{PHYS} was smaller than that for the other complexes (see Figure 3B) so the activation results for that complex contain their combined experimental uncertainties, and the D_E plot is slightly curved. Finally, the MePEG-750 tailed Co complex was examined but did not give stable voltammetry.

Consideration of Transport Results. Considering first the results for D_{PHYS}, Table 1 shows that the rates of physical self diffusion (D_{PHYS}) in the Co complex melts are increased by over 10^3-fold by increasing the length of the polyether chain attached to the bpy ligand. The viscosities are also very large and change in a parallel manner with polyether chain length (Table 1). These observations are not associated with phase changes in the melts since thermal measurements (*vide infra*, Figure 4) show that their glassing and melting transitions occur at lower temperatures than those employed. The rates of self diffusion in the undiluted melts also are from 10^2- to 10^4-fold smaller than are their diffusivities as dilute solutions (*vide infra*, Table 5) in the polyether solvent MePEG-400.

The chain length dependency of D_{PHYS} in Table 1 is opposite to results obtained for the diffusion of star polymers in high molecular weight matrices, which becomes slower as the

(17) Voltammetry of the MePEG-750 tailed complex was irreproducible and is not shown.

(18) The D_{PHYS} and D_{APP} results for the E_3M tailed complex are in good agreement with those in an earlier report.[3c] The D_{PHYS} and D_{APP} results for the MePEG-350 tailed complex cannot be compared to a previous report[3a] owing to the use of a supporting electrolyte there.

Table 1. Transport Constants for Metal Complex Melts

bpy tail	D_{PHYS}[a] (25 °C) (cm^2 s^{-1}) Co(III/II)	$E_{A,PHYS}$[b] (D_{PHYS}) (kJ mol^{-1}) Co(III/II)	η[c] (25 °C) (cP)	D_{APP}[a] (25 °C) (cm^2 s^{-1})		D_E[d] (25 °C) (cm^2 s^{-1})		$D_{E,COR}$[e] (25 °C) (cm^2 s^{-1})	
				Co(II/I)	Fe(III/II)	Co(II/I)	Fe(III/II)	Co(II/I)	Fe(III/II)
E_3M	$2.5 \pm 0.5 \times 10^{-13}$	79 ± 1	1.85×10^6	$3.0 \pm 0.5 \times 10^{-9}$	$1.9 \pm 0.3 \times 10^{-9}$	$3.0 \pm 0.5 \times 10^{-9}$	$1.9 \pm 0.3 \times 10^{-9}$	$1.1 \pm 0.2 \times 10^{-9}$	$8.4 \pm 0.9 \times 10^{-10}$
350	$1.3 \pm 0.2 \times 10^{-11}$	73 ± 3	1.60×10^4	$1.4 \pm 0.2 \times 10^{-9}$	$1.2 \pm 0.2 \times 10^{-9}$	$1.4 \pm 0.2 \times 10^{-9}$	$1.2 \pm 0.2 \times 10^{-9}$	$1.2 \pm 0.2 \times 10^{-9}$	$1.0 \pm 0.2 \times 10^{-9}$
550	$4.1 \pm 0.5 \times 10^{-10}$	54 ± 5	2.87×10^3	$1.9 \pm 0.4 \times 10^{-9}$	$6.0 \pm 0.6 \times 10^{-10}$	$1.5 \pm 0.5 \times 10^{-9}$	$1.8 \pm 1.1 \times 10^{-10}$	$1.3 \pm 0.4 \times 10^{-9}$	$1.2 \pm 0.7 \times 10^{-10}$

[a] Measured using chronoamperometry, fitting current−time transients to eq 2. Currents for the Co(II/III) reaction give D_{PHYS} values. [b] Average slopes of D_{PHYS} activation plots in Figure 3. For the MePEG-550 complex, the slope is taken over the lower studied temperature range, 298 to 323 K. [c] Average viscosity taken over a minimum of five rotation rates. [d] Calculated from eq 1. [e] Electronic migration correction applied, using parameters in Table 4.

Table 2. Electron Self Exchange Rate Constants in Undiluted Metal Complex Melts

	$k_{EX,COR}$, M^{-1} s^{-1}[a]		$E_{A,ET}$, kJ/mol[b]		$k_{EX}°$,[c] M^{-1} s^{-1}	
bpy tail	Co(II/I)	Fe(III/II)	Co(II/I)	Fe(III/II)	Co(II/I)	Fe(III/II)
E_3M[d]	$5.2 \pm 0.9 \times 10^5$	$4.0 \pm 0.5 \times 10^5$	29 ± 4	25 ± 2	$2 \pm 2 \times 10^{11}$	$1.8 \pm 0.9 \times 10^{10}$
350[e]	$6.7 \pm 1 \times 10^5$	$5.9 \pm 1 \times 10^5$	36 ± 3	34 ± 3	$2 \pm 2 \times 10^{12}$	$5 \pm 2 \times 10^{11}$
550[f]	$8.2 \pm 2 \times 10^5$	$7.4 \pm 4 \times 10^4$	35 ± 7		$1 \pm 3 \times 10^{12}$	

[a] $D_{E,COR} = k_{EX,COR}\delta^2C/6$, at 25 °C. [b] Slopes of activation plots as in Figure 3. [c] Intercepts of activation plots of D_E as in Figure 3, converted to rates by $D_{E,INT} = k_{EX}°\delta^2C/6$. [d] Density ρ, metal complex concentration C, and center-to-center spacing δ are 1.350 g/cm^3, 0.723 M, and 13.2 Å, respectively. [e] $\rho = 1.301$ g/cm^3, $C = 0.445$ M, $\delta = 15.5$ Å. [f] $\rho = 1.278$ g/cm^3, $C = 0.321$ M, $\delta = 17.3$ Å.

polymer star arm lengths are increased.[19] The chain lengths in these metal complex melts are too short to induce the entanglement effects that influence the transport of the star polymers.

The average center-to-center distances δ between the metal complexes in the melts were found from density measurements (Table 1, footnote) and are given for packing the molecules in a (fictitious) cubic lattice. The δ values are 13.2, 15.5, and 17.3 Å for the E_3M, MePEG-350, and MePEG-550 tailed complexes, respectively. A plot of these values against the number of ether monomer units/complex is linear with slope 0.525 Å/monomer unit and intercept 11.7 Å. This behavior indicates that each monomer unit adds a finite volume to the metal complex, which has an effective metal (non-tailed) bipyridine core size (diameter) of 11.7Å.

The polyether-tailed metal complexes can be regarded as relatively "hard" cores (the metal bipyridine complex) covered with a "soft", solvent-like shell (the attached polyether chain). From the above, the *average* polyether shell thickness is *ca.* 1.5, 3.8, and 5.6 Å in the three complexes, respectively, but with fluctuations and chain segmental rearrangements of the polyether chains, the polyether shell can be expected to be highly deformable. (The six chains attached to each complex should roughly approximate random coils.[20]) In the undiluted melts, the rate of physical diffusion of the bulky metal complex cores past one another should be strongly dependent on the dimensions of their "soft", deformable shells. We propose that the differing thicknesses of the polyether shells (i.e., different available deformable volumes) are the main source of the Table 1 differences in the D_{PHYS} values of the E_3M, MePEG-350, and MePEG-550 tailed Co complexes.

Deformations in the polyether shells are also reflected in the behavior of the D_{PHYS} activation plots in Figure 3 (■), which are strongly curved. This is consistent with known polymer electrolyte transport processes,[21] where curvature in activation plots is understood as coupling of the physical process to segmental motion of the polyether backbone. Deformation of metal complex polyether shells during diffusive translation of the metal complexes will require chain segmental rearrangements.

Pertinent questions regarding the electron transfer rates in the semisolid metal complex melts are the same as those asked in applying contemporary electron transfer theory[2,22] to fluid solution reactions, including the following: (i) are the reactions adiabatic, (ii) do the attached polyether chains impose a distance requirement for electron transfers, (iii) are work or entropy terms or precursor complex constants important, (iv) what terms comprise the free energy activation barrier, and (v) are the dynamics of solvent dipole reorientation important? The present results allow addressing of some of these important issues.

In the usual notation, the rate constant k_{EX} for a bimolecular electron transfer reaction is[22]

$$k_{EX} = k_A\kappa\nu k_N \tag{3}$$

where K_A is the donor−acceptor precursor complex formation constant, κ the electronic factor or transmission coefficient, ν the frequency factor, and k_N the nuclear factor which contains the free energy of activation. The nature of the electron transfers in the mixed valent metal complex melts affords some simplifications of these relations. First, since the reacting molecules are essentially in contact in the undiluted melt, work terms should not be important and are ignored in the calculation[23] of the precursor complex formation constant, $K_A = 1.05$ M^{-1}. Secondly, the reaction entropy and the entropy of activation (ΔS^*) are zero given that the reaction measured is an isotopic self-exchange process.[15,22b,24] Thirdly, it follows[22b] that the reaction enthalpies measured by the Arrhenius energy barriers $E_{A,ET}$ (Table 2) comprise estimates of the free energies of activation ΔG^* of the Co(II/I) and Fe(III/II) electron self exchanges. These, collectively, are circumstances favorable to evaluation of the pre-exponential terms $\kappa\nu$, as well as the reaction adiabaticity, and the Figure 3 Arrhenius plot intercepts ($k_{EX}°$, Table 2) may accept a rough interpretation in terms of the relation[24]

$$k_{EX} = K_A\kappa\nu\ \mathrm{EXP}\left[-\frac{\Delta G^*}{k_BT}\right] \tag{4}$$

where the reorganizational barrier energy $\lambda = 4\Delta G^* \approx 4E_A$ and the activation plot intercepts $k_{EX}°$ (Table 2) divided by K_A can be equated with $\kappa\nu$ (s^{-1}) using eq 3. A reaction with $\kappa\nu = 10^{13}$ s^{-1} is adiabatic,[22a] and one with $\kappa\nu = 10^{12}$ s^{-1} is typically taken as adiabatic.[22] The Table 2 results indicate that the Co(II/I) electron transfer reactions in the Co complex melts are if not adiabatic nearly so, and that the Fe(III/II) electron transfers approach adiabaticity.

The conclusion regarding adiabaticity is consistent with estimations[25] of the electronic matrix element coupling term H_{AB}

(19) Shull, K. R.; Kramer, E. J.; Felters, L. J. *Nature* **1990**, *345*, 790.

(20) (a) Sperling, L. H. *Introduction to Physical Polymer Science*, 2nd ed.; John Wiley & Sons, Inc.: New York, 1992; pp 173−178. (b) The end-to-end distance (r_f) of a freely jointed polymer chain may be calculated using the following:[20a] $r_f^2 = Cl^2x$, where C is the characteristic ratio (≃4.1 for polyethlyene oxide), l is the length of the bond, and x is the number of bonds in the chain. For the MePEG-350 chain, r_f is estimated to be 12 Å. While the use of C in the calculation approximates the excluded volume for the chain, this method neglects the bond angle restrictions on the conformation of the chain.

(21) (a) Gary, F. M. *Solid Polymer Electrolytes, Fundamentals and Technological Applications*; VCH Publishers, Inc.: New York, 1991. (b) MacCallum, J. R.; Vincent, C. A. *Polymer Electrolyte Reviews*; Elsevier Applied Science: Oxford, UK, 1989; Vols. 1 and 2.

(22) (a) Marcus, R. A.; Sutin, N. *Biochim. Biophys. Acta* **1985**, *811*, 265. (b) Marcus, R. A.; Siddarth, P. In *Photoprocesses in Transition Metal Complexes, Biosystems, and Other Molecules*; Kochanski, E., Ed., Kluwer Academic Publishers: Dordrecht, The Netherlands, 1992. (c) Sutin, N. *Acc. Chem. Res.* **1982**, *15*, 275. (d) Sutin, N. *Prog. Inorg. Chem.* **1983**, *30*, 441.

(23) The calculation of K_A is based on the equation[22d]

$$K_A = 4\pi N_A\bar{r}^2\delta\bar{r}/10^3$$

where the center-to-center distance, $\bar{r}$, is taken as that for the E_3M tailed complex, 13.2 Å, and $\delta\bar{r}$ is taken[22d] as 0.8 Å.

(24) Newton, M. D.; Sutin, N. *Annu. Rev. Phys. Chem.* **1984**, *35*, 437.

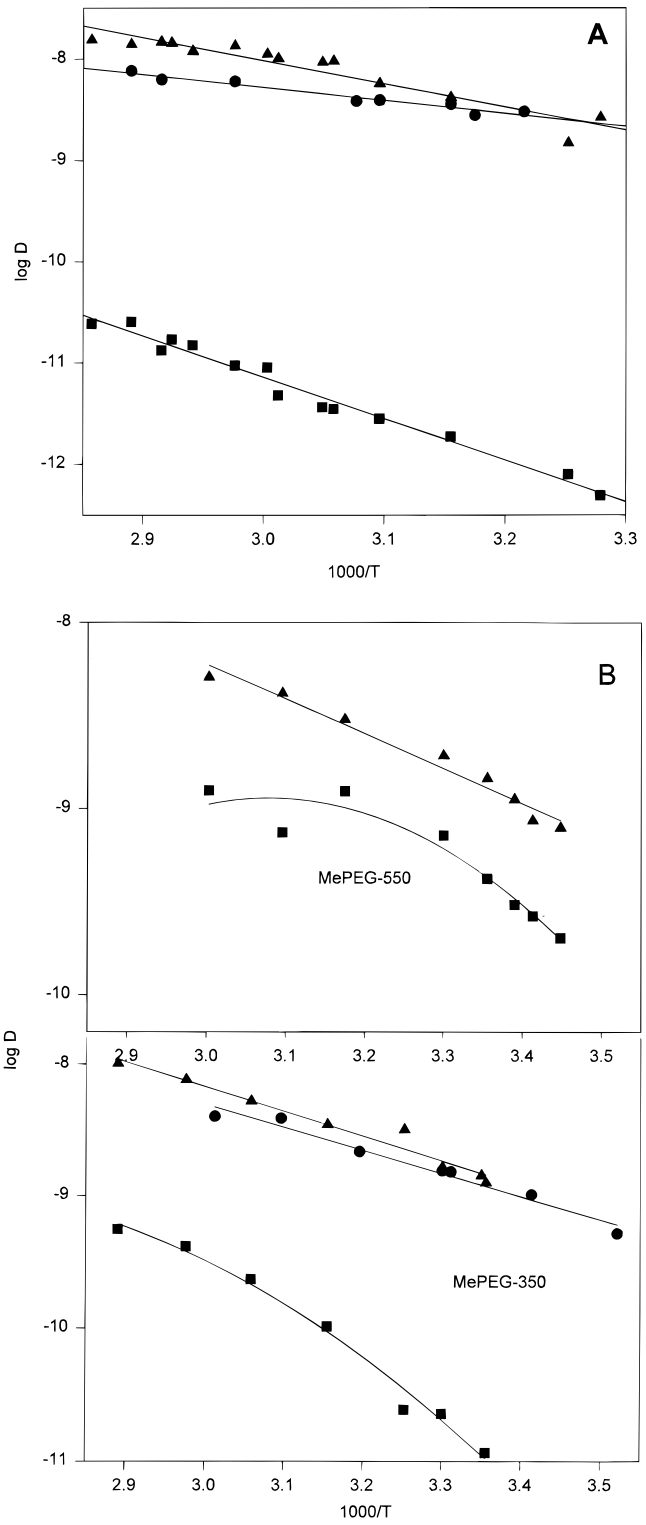

Figure 3. Activation plots of D_E (=D_{APP} − D_{PHYS}) for $Fe^{3+/2+}$ (●) and $Co^{2+/1+}$ (▲) reactions, and of D_{PHYS} for $Co^{3+/2+}$ (■) reaction: panel A, E_3M tailed melts; panel B, MePEG-350 and MePEG-550 tailed melts.

and with the behavior of the 25 °C rate constants $k_{EX,COR}$ in Table 2. The rate constants $k_{EX,COR}$ change little with increasing polyether chain length for the Co(II/I) reaction and do not vary systematically for the Fe(III/II) reaction. *The lack of a significant dependence of k_{EX} on the polyether chain length is a meaningful result since it indicates the absence of electron tunneling effects.* If the metal complex cores were constrained to undergo electron transfers at distances prescribed by the thicknesses (*vide supra*) of their surrounding, attached polyether shells, the electron transfer rate constants should *decrease* with increasing polyether chain length. Invoking the usual exponential rate−distance relationship,[22a] the decrease in k_{EX} would be *ca*. 10- and 60-fold for the MePEG-350 and MePEG-550 tailed complexes, respectively, relative to the E_3M tailed complexes. These changes are large enough to be readily detectable, and are not seen in the Table 2 data. The electron transfers in the melts must therefore occur by reasonably close approach of the metal complex cores to one another, and by inference the metal complex cores must move within their soft polyether shells on time scales faster than the frequencies at which electron transfers occur. This result is entirely consistent with that of the physical diffusion picture, i.e., that the metal complexes are comprised of hard metal bipyridine cores and soft, deformable polyether shells. The absence of significant electron transfer distance effects is also consistent with the near-adiabaticity of the reactions indicated by the magnitudes of the $k_{EX}°$ results in Table 2.

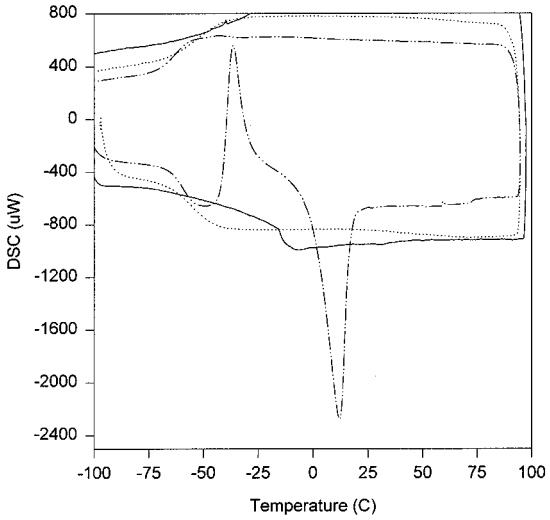

Figure 4. Differential scanning calorimetry traces for undiluted $[Co(bpy(CO_2E_3M)_2)_3](ClO_4)_2$ (—) $[Co(bpy(CO_2MePEG\text{-}350)_2)_3](ClO_4)_2$ (− −), and $[Co(bpy(CO_2MePEG\text{-}550)_2)_3](ClO_4)_2$ (—••—).

The free energy barrier ΔG^*, in the context of Marcus theory,[22] is composed of outer- and inner-sphere reorganizational energies. The former, normally, reflects the energetics of dipolar reorientation of the solvation shell of the reactants, as given by

$$\Delta G^*_{OS} = \frac{N_A e^2}{16\pi}\left[\frac{1}{2a_1} + \frac{1}{2a_2} - \frac{1}{R}\right]\left[\frac{1}{\epsilon_{OP}} - \frac{1}{\epsilon_S}\right] \qquad (5)$$

where a_1 and a_2 are the reactant radii, R their center-to-center separation, and ϵ_{OP} and ϵ_S the solvent optical and static dielectric constants, respectively. The inner-sphere barrier represents nuclear motions within the reactants themselves and is typically discussed in terms of differences between the reactants' metal−ligand bond lengths.

It is instructive to imagine that the polyether chains attached to a metal bipyridine core serve as its "solvent shell", and on that basis to evaluate ΔG^*_{OS} for the Co(II/I) and Fe(III/II) reactions using eq 5. Assuming that the polyether chains have the dielectric properties of an unattached ether solvent, the

(25) Were the melt electron transfers analyzed as non-adiabatic, their electronic matrix element coupling terms H_{AB} could be estimated from the relation[22] $\kappa\nu = 2\pi|H_{AB}|^2/\hbar[4\pi\lambda k_B T]^{1/2}$. Using values from Table 2 for $\kappa\nu$ (=$k_{EX}°/K_A$) and λ (=$4E_{A,ET}$), the obtained H_{AB} values range from 29 to 110 cm^{-1} for the Co(II/I) reaction and 8 to 72 cm^{-1} for the Fe(III/II) reaction. These large coupling terms are more consistent with adiabatic than non-adiabatic behavior.

Table 3. Ionic Conductivities and Glass Transition Temperatures of Undiluted Metal Complex Melts

bpy tail	metal	σ_{ION} (Ω^{-1} cm^{-1}) (25 °C)	$E^*_{A,ION}$ Arrhenius (kJ/mol)[a]	$E_{A,ION}$ VTF (kJ/mol)	T_O (K)	T_G (°C)
E_3M	Co	$1.39 \pm 0.01 \times 10^{-7}$	66 ± 2	11.3 ± 0.6	188 ± 3	−25
	Fe	$1.39 \pm 0.01 \times 10^{-7}$	67 ± 3	11.7 ± 0.7	190 ± 3	−22
MePEG-350	Co	$6.40 \pm 0.03 \times 10^{-7}$	48 ± 2	9.0 ± 1.0	187 ± 7	−56
	Fe	$6.86 \pm 0.04 \times 10^{-7}$	53 ± 2	10.5 ± 0.5	181 ± 3	−48
MePEG-550	Co	$4.57 \pm 0.02 \times 10^{-6}$	33 ± 2	6.5 ± 0.6	186 ± 5	−61
	Fe	$4.08 \pm 0.02 \times 10^{-6}$	34 ± 2	6.2 ± 0.4	188 ± 3	−59
MePEG-750	Co	$1.31 \pm 0.01 \times 10^{-5}$	26 ± 1	*b*		−61

[a] Average slopes of σ_{ION} activation plots (Figure 5) using data above temperatures of 298 K. [b] VTF fit not performed because of insufficient temperature range.

calculation for the Co(II/I) reaction gives $\Delta G^*_{OS} = 9$ kJ/mol.[26] This value, and those from all other calculations assuming physically plausible parameters in eq 5, are far smaller than the experimental activation energies for the electron transfers in the melts.

The conclusion may be drawn that the Fe(III/II) and Co(II/I) metal complex melt electron transfers involve a large "inner-sphere"-like barrier energy, which seems to be larger for longer attached polyether chains. Large activation barriers were also obtained in a related study of polyether tailed melts in which $[Ru(bpy)_3]^{2+/3+}$ and $[Ru(bpy)_3]^{2+/1+}$ electron transfers occur.[27] The metal−ligand bond distances in the unsubstituted forms of all these metal bipyridine complexes are nearly the same in their different oxidation states,[22,28] and distortions of the metal−ligand distances or of the tailed bipyridine ligands themselves in the melt complexes would be somewhat surprising. In other words, an inner-sphere barrier of the classical kind, involving the metal complex core as we have termed it above, is not expected in these reactions.

The ambiguity posed, of course, by the preceding discussion is that the polyether chains are *not free solvent molecules but are attached to the metal bipyridine cores, and their rearrangements of nuclear coordinates as part of the electron transfer event contribute an "inner-sphere"-like barrier term.* We should emphasize that the label "inner-sphere" is used solely to distinguish the barrier contribution from that anticipated from eq 5, and indeed an alternative phrasing is possible.[29] The hypothesis of coupling of the bpy ligand to its "solvent shell" blurs the usual distinctions between the energetics of the reactants' vibrational modes and those of dipolar reorientations of the surrounding solvent, and suggests that the energy barrier effects of "solvent"−ligand coupling can be quite large. Current experiments are aimed at further evaluation of the coupling hypothesis.

Our previous investigations[3,4] of electron self exchange kinetics of well-defined redox couples in solid and semisolid polymeric and melt phases have rather uniformly led to room temperature rate constants that were smaller, sometimes substantially so, than the rate constants for the corresponding redox moieties dissolved in fluid solutions. This observation is repeated here; the 25 °C k_{EX} values in Table 2 are several orders of magnitude slower than the fluid solution $[Co(bpy)_3]^{2+/1+}$ and $[Fe(bpy)_3]^{2+/3+}$ kinetics.[18,30] The more complete analysis afforded above, through polyether chain length and temperature variations, shows in reference to eq 4 that, at least in the present examples, this kinetic slowing arises more from increased energy barriers than from diminished pre-exponential terms.

Finally, comparison of the activation barriers for the electron transfer and for physical diffusion is complicated because of the curvature in the latter's activation plots (Figure 3 (■)). In general, at lower temperatures the *average* slopes of the D_{PHYS} activation plots ($E_{A,PHYS}$, Table 1) exceed those of the electron transfer activation plots. This is reasonable since the chain rearrangements required to bring the metal complex cores together within their polyether "solvent" shell (and to satisfy the dipolar reorientation requirements) should be energetically less substantial than the deforming chain rearrangements needed to allow the cores to physically move past one another.

Thermal Measurements and Ionic Conductivities. Well-defined glassing transitions were observed by differential scanning calorimetry (Figure 4) for each of the metal complex melts; values of T_G are given in Table 3. The glassing temperature decreases strongly with increasing chain length which is consistent with the variation of D_{PHYS} with polyether chain length (*vide supra*, Table 1). The E_3M and MePEG-350 tailed complexes exhibit only glassing (i.e., no melting) transitions; the MePEG-750 (not shown) and MePEG-550 (Figure 4) tailed complexes exhibit progressive exo- and endotherms at *ca.* −28 and 12 °C in the heating curves. These temperatures are below those used for transport rate measurements, so the metal complexes are uniformly in the melt phase for all those measurements.

The intrinsic ionic conductivities of the metal complex melts add to our understanding of transport in these novel materials, and also aid evaluation of potential distortions of D_{APP} measurements by migration effects. Classical transport of electrolyte ions, such as those of $LiClO_4$, occurs in polyether polymer electrolytes for the cation by successive coordination/release by a progression of ether oxygens in the polyether matrix.[21] The microscopic transport details for the anion are not as clearly established. In the present materials, movement of the metal bipyridine cation is coincident with that of the ether chains (and of their deformation).

Table 3 shows results for ionic conductivity, σ_{ION} , in the undiluted metal complex metals. As expected, σ_{ION} is the same for Co and Fe complexes bearing the same polyether tail, and like D_{PHYS}, σ_{ION} increases with increasing polyether chain length but to a much smaller degree. The difference in the chain length dependencies of D_{PHYS} and of σ_{ION} to some extent reflects the lowering of ion concentrations with longer polyether chain lengths (see footnotes D−F, Table 2), but likely also reflects differences in relative mobilities of the metal complex cation and its anion (*vide infra*).

Activation plots for σ_{ION} are strongly curved (Figure 5) as typical[21] of transport processes involving strong coupling to polyether chain segmental motions. The activation plots were

(26) We use the values $a_1 = a_2 = 6.6$ Å and $R = 13.2$ Å and from ref 3b $\epsilon_{OP} = 2.13$ and $\epsilon_S = 9.16$.

(27) Masui, H., University of North Carolina at Chapel Hill, manuscript in preparation.

(28) Brunschwig, B. S.; Creutz, C.; Macartney, D. H.; Sham, T.-K.; Sutin, N. *Faraday Discuss. Chem. Soc.* **1982**, *74*, 113.

(29) An alternative but functionally equivalent description is that the reaction responds to the reorientational *dynamics* for repolarization of its "solvent shell"[2d−f] and that the experimental activation energy includes that for the attached polyether chain reorientation (i.e., the thermal barrier of dipolar longitudinal relaxation of the attached chains).

(30) Chan, M.-S.; Wahl, A. C. *J. Phys. Chem.* **1978**, *82*, 2542.

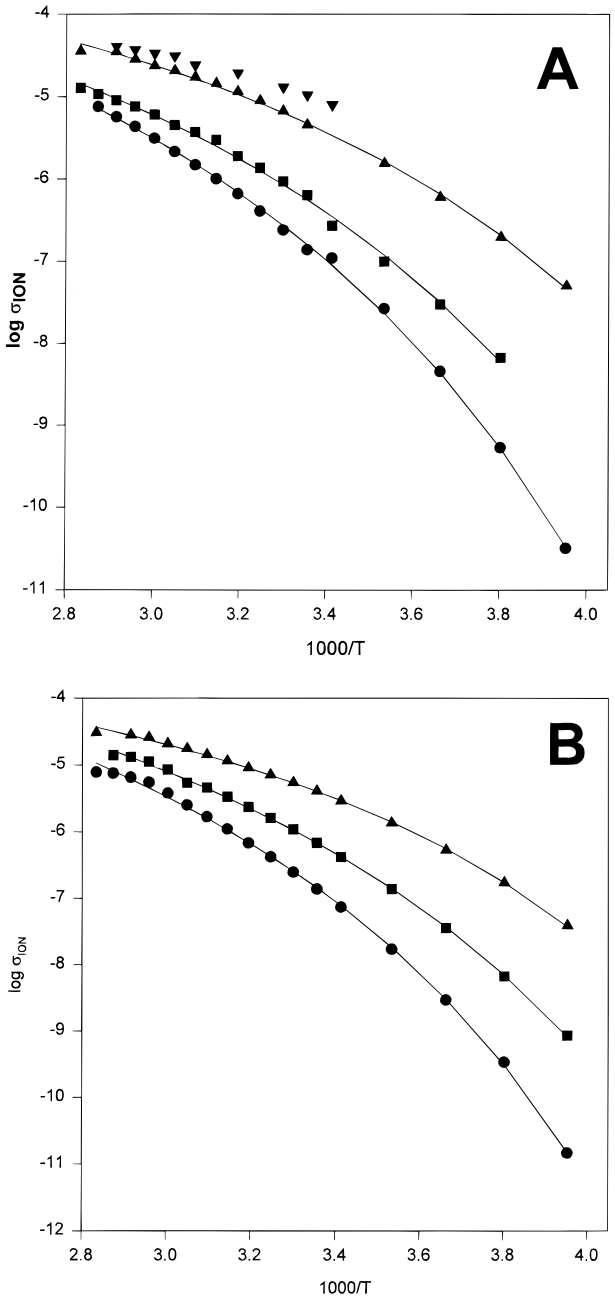

Figure 5. Activation plots of σ_{ION} with VTF fit (—): E_3M tailed (●), MePEG-350 tailed (■), MePEG-550 tailed (▲), and MePEG-750 tailed (▼) melts for panel A, Co complexes, and panel B, Fe complexes.

fitted to the Vogel−Tamman−Fulcher (VTF) equation:[31]

$$\sigma_{ION} = \frac{A'}{T^{1/2}} \mathrm{EXP}\left[-\frac{E_{A,ION}}{R(T - T_O)}\right] \qquad (6)$$

where T_O is the reduced temperature and A' a parameter related to the number of charge carriers. The fitting results (Table 3) show that the VTF energy barrier $E_{A,ION}$ decreases for the longest chain length and the reduced temperature is nearly constant.

Comparing the barriers for σ_{ION} and D_{PHYS} in terms of the average slopes of their activation plots over a common temperature range (i.e., above 298 K), the barriers for D_{PHYS} (Table 1, $E_{A,PHYS}$) are much larger than those for σ_{ION} (Table 3, $E^*_{A,ION}$). Remembering that D_{PHYS} reflects transport of the metal complex cation, the difference in barrier energy means that the ClO_4^- counterion is intrinsically more mobile, a result consistent with those for transference number, below.

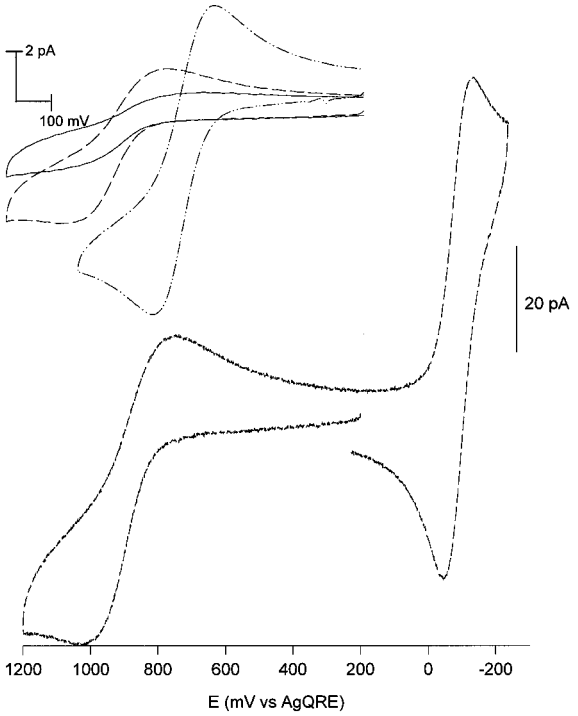

Figure 6. Cyclic voltammogram (25 mV/s) for 2.3 mM $[Co(bpy(CO_2E_3M)_2)_3](ClO_4)_2$ in 1.5 M $LiClO_4$ in MePEG-350 at a 12.5 mm radius Pt microdisk electrode. Inset: expanded Co(III/II) voltammograms (25 mV/s) for dilute solutions of $[Co(bpy(CO_2C_2H_5)_2)_3]^{2+}$ (—••—), $[Co(bpy(CO_2E_3M)_2)_3]^{2+}$ (— —), and $[Co(bpy(CO_2MePEG\text{-}350)_2)_3]^{2+}$ (—).

Consideration of Migration. Transport driven by electrical gradients (migration) can cause errors in diffusion measurements using eq 2, which assumes that only concentration gradients are important. Physical diffusion rates in the melts will be retarded if the metal bipyridine cations have large transference numbers (i.e., the measured D_{PHYS} is smaller than the real value), and electron self exchange rates enhanced if the counterion diffusivity (D_{ClO_4}) is significantly less than that of the electron (i.e., the measured D_E is larger than the real value). Evaluation of D_{ClO_4}, central to analysis of these effects, is done using the Nernst−Einstein equation:[32a]

$$\sigma_{ION} = \frac{F^2}{RT}[z^2_{ClO_4} D_{ClO_4} C_{ClO_4} + z^2_{M^{2+}} D_{M^{2+}} C_{M^{2+}}] \qquad (7)$$

where z_i, D_i, and C_i are ionic charge, diffusion coefficient, and concentration, respectively. Since σ_{ION} and D_{PHYS} are known (Tables 1 and 3), D_{ClO_4} can be calculated from eq 7; the resulting (25 °C) values are given in Table 4.

Considering ionic migration, Table 4 shows that D_{ClO_4} throughout is larger than D_{PHYS} (Table 1). Table 4 gives the ClO_4^- transference numbers calculated from these results. In the E_3M and MePEG-350 tailed melts, the predominant ionic charge flow is carried by the anion, and correspondingly the effect of ionic migration on measured D_{APP} values is negligible in these melts. In the case of the MePEG-550 tailed complex melts, the transference results suggest that some ionic migration

(31) (a) Vogel, H. *Phys. Z.* **1921**, *22*, 645. (b) Tammann, G.; Hesse, W. *Z. Anorg. Allg. Chem.* **1926**, *156*, 245. (c) Fulcher, G. S. *J. Am. Ceram. Soc.* **1925**, *8*, 339.

(32) (a) Bard, A. J.; Faulkner, L. R. *Electrochemical Methods*; John Wiley & Sons: New York, 1980; pp 227−231. (b) In ref 32a, pp 227. (c) Nicholson, R. S. *Anal. Chem.* **1965**, *37*, 1351. (d) Nicholson, R. S.; Shain, I. *Anal. Chem.* **1964**, *26*, 704.

Table 4. Analysis of Migration Effects

	D_{ClO_4} ($cm^2\ s^{-1}$)		t_{ClO_4}[a]		D_{ClO_4}/D_E	
bpy tail	Co(II/I)	Fe(III/II)	Co(II/I)	Fe(III/II)	Co(II/I)	Fe(III/II)
E_3M	$2.5 \pm 0.4 \times 10^{-11}$	$2.5 \pm 0.3 \times 10^{-11}$	0.98 ± 0.08	0.98 ± 0.08	0.0083 ± 0.0006	0.013 ± 0.001
MePEG-350	$1.7 \pm 0.3 \times 10^{-10}$	$1.8 \pm 0.4 \times 10^{-10}$	0.88 ± 0.03	0.89 ± 0.03	0.117 ± 0.003	0.15 ± 0.01
MePEG-550	$1.1 \pm 0.3 \times 10^{-9}$	$8.5 \pm 0.9 \times 10^{-10}$	0.55 ± 0.01	0.52 ± 0.01	0.72 ± 0.01	4.7 ± 0.1

[a] t_{ClO_4} is the transference number for the ClO_4^- counterion.

Table 5. Voltammetric Results in Dilute Metal Complex Solutions in 1.5 M $LiClO_4$/MePEG-350 Polymer Electrolyte

metal complex	D_{PHYS} ($cm^2\ s^{-1}$)	$k°$ ($cm\ s^{-1}$)	r_H (app) (Å)
$[Co(bpy)_3](ClO_4)_2$	$1.6 \pm 0.3 \times 10^{-8}$	$3 \pm 0.1 \times 10^{-4}$	9.9
$[Co(bpy(CO_2C_2H_5)_2)_3](ClO_4)_2$	$9 \pm 0.2 \times 10^{-9}$	$3 \pm 0.3 \times 10^{-5}$	19
$[Co(bpyE_3M)_3](ClO_4)^2$	$7 \pm 0.2 \times 10^{-9}$	$8 \pm 0.9 \times 10^{-6}$	23
$[Co(bpyMePEG350)_3](ClO_4)_2$	3.6×10^{-9}	n.a.[a]	45

[a] n.a. = not available.

of the metal complex may occur, which would slightly depress the measured D_{PHYS}. It is important to note that our use of eq 7 ignores ionic association, and the calculated D_{ClO_4} values are actually thus lower limits.

Electronic migration refers to electron diffusivity (through self exchanges) exceeding that of the charge-compensating counterions (i.e., $D_{ClO_4}/D_E \ll 1$). As described by Andrieux and Saveant,[33] the ensuing potential gradient across the mixed valent layer around the electrode accelerates electron transfers. The ratio D_{ClO_4}/D_E for the different melts (Table 4) shows that electronic migration effects should occur in the E_3M and MePEG-350 tailed melts; these were corrected by application of the appropriate theoretical working curves[34] to produce the $D_{E,COR}$ results in Table 1. By comparison to the raw D_E values, the electronic migration corrections ranged from 3-fold to negligible.

The above analysis shows that, overall, the effects of ionic and electronic migration on the diffusion measurements in Table 1 are small. For this reason, the activation analysis in Figure 3 uses D_E, not $D_{E,COR}$.

Voltammetry of Tailed Co Complexes as Dilute Solutions in Polyether. A brief study was conducted of solutions of polyether tailed and untailed Co complexes in 1.5 M $LiClO_4$/MePEG-350 polymer electrolyte. Electron self exchange is rendered unimportant at low concentrations of the redox species and physical diffusion becomes the dominant transport mode (eq 1). Microelectrode voltammetry is shown in Figure 6. The Co(III/II) wave is quasireversible whereas that for the Co(II/I) reaction is relatively reversible; considering these differences, the oxidation and reduction peak currents are very similar, meaning charge transport occurs by physical diffusion alone.

Diffusion coefficients measured by chonoamperometry are given in Table 5. The results reveal systematic decreases in D_{PHYS} in proceeding from the untailed complex to the ethyl ester to the E_3M and MePEG-50 tailed complexes; these changes are in the opposite direction to those in the melts (D_{PHYS},Table 1). A decrease in diffusivity is expected for large molecules in dilute solution, according to the Stokes−Einstein equation:[35]

$$D = \frac{k_B T}{6\pi\eta r_H} \tag{8}$$

where k_B is Boltzmann's constant, η is viscosity (132.3 cP in MePEG-350 solutions), and r_H is the hydrodynamic radius of the diffusant molecule. Calculated r_H values (Table 5) are slightly larger than expected[36] for the $[Co(bpy)_3]^{2+}$ complex but the apparent radii are much larger for the ethyl ester, E_3M, and MePEG-350 tailed complexes (compare to the δ of the undiluted states, footnotes *d*−*f*, Table 1).

It was possible to measure the heterogeneous electron transfer kinetics for three of the Co(III/II) reactions in MePEG-350 solutions using the classical Nicholson−Shain treatment for quasireversible systems.[29b−d] (This was not done for the voltammetry in Figure 1 which requires special attention to resistance effects and will be treated elsewhere.[9]) The Co(III/II) voltammetry for polyether chains other than the E_3M case was too poorly defined for rate measurements. The results (Table 5) for $k°$ were invariant with potential scan rate,[37] and for untailed $[Co(bpy)_3]^{2+/3+}$ agree with those previously obtained in a Me_2PEG-400 solution.[3b,38] The esterification of the bipyridine ligand and the attachment of an E_3M tail causes substantial slowing of the heterogeneous electron transfers. The reason(s) are unclear. Steric or electron transfer distance effects might produce rate changes in the direction seen, but do not seem plausible given the behavior of the Co(II/I) electron transfers in the undiluted melts where the attached chains had only minor if any effect on the 25 °C rate constants. The 10-fold difference in $k°$ between the $[Co(bpy)_3]^{2+/3+}$ and the $[Co(bpy(CO_2C_2H_5)_2)_3]^{2+/3+}$ ions is especially implausible as a distance effect alone.

Acknowledgment. This research was supported in part by grants from the Department of Energy and the National Science Foundation. M.E.W. acknowledges her undergraduate professors from the Chemistry Department of St. John Fisher College, Rochester, NY.

JA962531M

(33) Andreiux, C. P.; Saveant, J. M. *J. Phys. Chem.* **1988**, *92*, 6761.

(34) From working curves[33] using $-(\gamma + 1) = 2$, $n/z_c = +1$ for Fe(III/II), and $n/z_c = -1$ for Co(II/I).

(35) Atkins, P. W. *Physical Chemistry, 4th ed.;* W. H. Freeman & Co.: New York, 1990.

(36) From ref 22a, for $Co(bpy)_3^{2+}$ $r = 7$ Å.

(37) For example, $[Co(bpy)_3](ClO_4)_2$ at scan rates of 100, 125, 150, 200, 250, 300, 400, 450, and 500 mV/s gave $k°$ values of 2.9×10^{-4}, 2.7×10^{-4}, 2.6×10^{-4}, 3.1×10^{-4}, 3.0×10^{-4}, 3.0×10^{-4}, 3.0×10^{-4}, 2.9×10^{-4}, and 2.9×10^{-4} cm s^{-1}, respectively. The $[Co(bpyE_3M)_3](ClO_4)_2$ complex at scan rates of 10, 20, 25, 30, and 40 mV/s gave $k°$ values of 7.7×10^{-6}, 8.2×10^{-6}, 5.7×10^{-6}, 7.8×10^{-6}, and 6.5×10^{-6} cm s^{-1}, respectively.

(38) The reported[3b] $D_{APP} = 3.3 \pm 0.2 \times 10^{-8}$ $cm^2\ s^{-1}$ and $k°= 2.1 \pm 0.9 \times 10^{-4}$ in a solution of Me_2PEG-400 containing 1.5 M $LiClO_4$.